International Journal of Heat and Technology
Vol. 43, No. 4, August, 2025, pp. 1567-1572
Journal homepage: http://iieta.org/journals/ijht

Manufacturing of Zinc Oxide Nanoparticles for Medical Applications

Ali M. Ahmed[1*], Russul M. Shehab[2], Ghaidaa A. Khalid[2], Mustafa Adnan Zaidan[3]

[1] College of Medicine, Mustansiriyah University, Baghdad 10001, Iraq
[2] Electrical Engineering Technical College, Middle Technical University, Baghdad 10001, Iraq
[3] Medical Technical College, Al-Farahidi University, Baghdad 10001, Iraq

Corresponding Author Email: ali.majeed@uomustansiriyah.edu.iq

https://doi.org/10.18280/ijht.430433

Received: 2 June 2025
Revised: 24 July 2025
Accepted: 5 August 2025
Available online: 31 August 2025

Keywords:
zinc oxide nanoparticles, biomedical applications, antibacterial activity, laser ablation

ABSTRACT

The pulsed laser ablation in liquid (PLAL) method was used to synthesize ZnO NPs, which were subsequently characterized for their structural, optical, and antibacterial properties. FE-SEM showed the nanoparticles with needle morphology, of size 20-50 nm, which was also confirmed by XRD analysis with high crystallinity of 28.09-31.86 nm for average crystallite size. The absorption band at 284.5 nm revealed in UV-Vis spectroscopy was characteristic of the use of ZnO NPs. Antibacterial activity testing was assessed by the well diffusion assay in which inhibition zones of up to 25 ± 1.2 mm for S. aureus and 20 ± 1.5 mm for E. coli were seen at 50 µL (50 mg/10 mL) concentration. Results demonstrate that ZnO NPs can act as effective antibacterial agents by damaging bacterial membranes. Compared to the previous studies, which focused on spherical shapes or chemically synthesized ZnO NPs, however, this work can show the macroporous fabrication of high-purity, needle-shaped ZnO NPs with a single step, eco-friendly pulsed laser ablation in liquid technique, leading to higher antibacterial activity by enhancing surface area reactivity and crystallinity. The results of this study indicate that the pulsed laser ablation in liquid method is a suitable way to produce high-purity ZnO NPs for potential use in biomedical fields, including antimicrobial and wound healing applications.

1. INTRODUCTION

Zinc oxide nanoparticles (ZnO NPs) are multifunctional materials with advantages as it is extremely photostable, cover a large range of radiation absorption, and the electrochemical coupling coefficient is quite high and chemically stable [1-3]. Because of its direct wide band gap energy (3.37 eV), high thermal and mechanical stability at room temperature, large exciton binding energy (60 meV) and its perspectives in the electronics, optoelectronics, and laser technology ZnO has high scientific and technical interest to the use ZnO as a sensor, a converter, a photocatalyst and an energy producer for syntheses of hydrogen devices because it possesses pyroelectric and piezoelectric characteristics [4-6]. Its low toxicity, biocompatibility, and biodegradability make it an intriguing material for pro-ecological and biomedical systems. Because of its hardness, stiffness, and piezoelectric constant, it is an essential part of ceramic production [7, 8].

For the synthesis of ZnO nanoparticles, a variety of techniques have been reported in the literature [9, 10]. These methods, which fall into either the chemical or physical categories, include spray conversion processing, sol-gel, chemical vapour deposition, nanolithography, and precipitation [11, 12]. Metal oxide nanoparticles have undergone substantial research to determine their potential as an antibacterial agent. When nanoparticles are deposited on the surface of bacteria or accumulate in the cytoplasm or periplasm, membrane rupture and disorder ensue [13]. According to a similar theory, ZnO NPs can stop the growth of bacteria by rupturing their membranes, which raises membrane permeability and results in the buildup of nanoparticles in the bacterial membrane and cell cytoplasm. precipitation, or chemical vapor deposition, the pulsed laser ablation in liquid (PLAL) technique offers several advantages. It is a simple, one-step and eco-friendly method that avoids the use of toxic reagents or complex reaction conditions, while simultaneously ensuring high purity of the obtained nanoparticles. Moreover, PLAL allows precise control over nanoparticle morphology and size distribution by tuning laser parameters, which is challenging to achieve with chemical synthesis. These features make PLAL highly attractive for biomedical applications, where purity and controlled morphology directly affect biocompatibility and antibacterial performance. Recent reports [5, 11-13] as well as more recent studies [14, 15] have emphasized the growing importance of PLAL in producing ZnO NPs with enhanced structural and antimicrobial properties, confirming its timeliness as a sustainable nanofabrication approach [16].

However, most previous studies relied on chemical synthetic methods such as complex procedures, toxic reagents, or had uncontrolled particle morphology. Additionally, very little attention has been paid to the formation of ZnO nanoparticles with well-defined shapes, i.e., needles, using pulsed laser ablation in liquid (PLAL), and testing of their

antibacterial activity. However, there is a gap to bridge in using PLAL to produce high-purity ZnO NPs in a simple, clean, and controlled manner, and to examine their structural and antibacterial properties in detail [17]. The objective of this study is to create needle-shaped, high-purity ZnO nanoparticles utilizing an environmentally friendly, one-step pulsed laser ablation in liquid (PLAL) approach in light of these constraints. A structural, optical, and antibacterial evaluation of the produced nanoparticles will be conducted. It is anticipated that this method will provide ZnO NPs with higher surface activity and crystallinity, providing better antibacterial efficacy than particles that are traditionally manufactured. The results of this investigation may aid in the creation of safer and more efficient nanomaterials for use in biological applications.

2. MATERIALS AND METHODS

PLAL was used to synthesize ZnO nanoparticles from a zinc target (1 mm thickness, 99.99% purity). A glass vessel containing 5 mL of deionized water and containing a piece of zinc metal is placed at the bottom. After 10 minutes of ultrasonic cleaning in acetone, the metal was rinsed with distilled water to get rid of the impurities. The source was an Nd: YAG laser with a Q-switch (first harmonic) to ablate the Zn target vertically operated at 532 nm, and it delivered 200 pulses with an energy of 600 mJ, each of 8 ns duration, at a rate of 10 Hz, ablation taking 4 minutes. The ablation fluency was about 1.4 J/cm^2. In this case, the laser beam passed through the lens but was focused on the lens itself at a distance of 4 cm from the zinc bulk (focal length of the lens = 12 cm). To create uniform nanoparticles, the vessel was rotated. The schematic diagram of the employed equipment is displayed in Figure 1 [18].

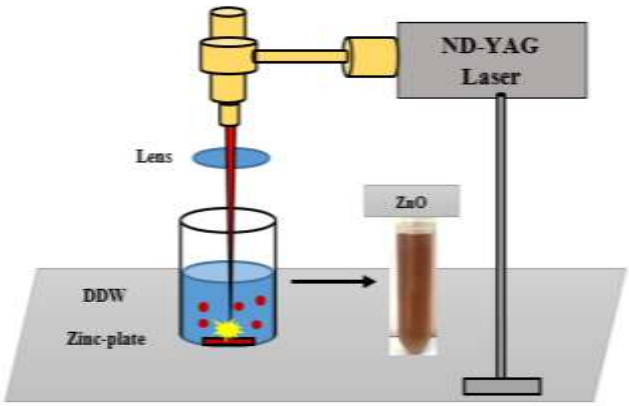

Figure 1. Ablation using pulsed laser in liquid techniques for the formation of ZnO colloidal nanoparticles

To test both the gram-positive (S. aureus) and gram-negative (E. coli) bacteria, the well diffusion assay method was applied to determine the antibacterial properties of zinc oxide nanoparticles. The implant's surface had a 6 mm diameter hole drilled through with a 6 mm diameter sterile hole drilled in a bacterial suspension of 20 ml per cell, which was kept in a medium (muller hinton agar) and then planted in dishes.

Each hole contained 50 µl of the extracts that were produced for the drill. Figure 2 illustrates how ZnO affects the manufactured bacteria's cells [19]. The extract's effectiveness was examined following a 24-hour incubation period at 37° using the area of a hole at 37° in milliliters of inhibition. The following formula is used to determine the scavenging ability [20]:

$$\% \text{ Inhibition } = 100 \times \left(\frac{A-B}{A}\right) \quad (1)$$

where, the inhibition percentage is denoted by I (%), the Control reaction absorbance is denoted by A, and the test substance sample absorbance is denoted by B.

Two different species of bacteria were then exposed to the produced NPs antimicrobial activities, the first is the bacteria that cause wounds and burns, E. coli, and the second is the bacteria that infect the intestinal tract (intestines), S. aureus.

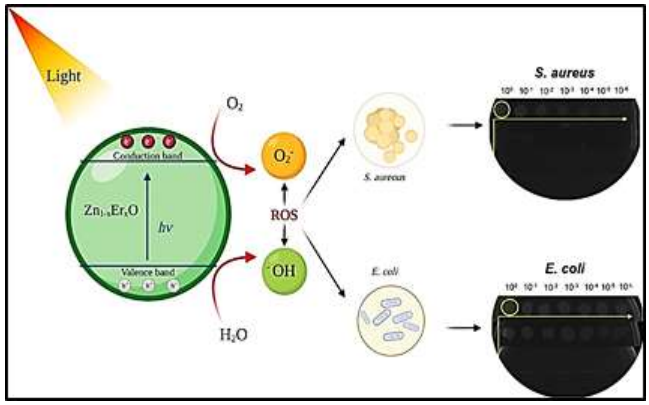

Figure 2. Presents a schematic illustration of ZnO's antibacterial action [18]

The structure and morphology of ZnO NPs were assessed using a TESCAN MIRA3 field emission scanning electron microscope (FE-SEM). To identify impurities and phases, X-ray diffraction examination was performed using a Philips X'pert diffractometer that used Cu-kα (λ = 1.54 Å) radiation running at 40 kv and 30 mA. The Scherrer method and elemental mapping were used to estimate the crystallite sizes of the samples. Optical characterisation was performed using a UV-Vis spectrometer (Analytikjena SPECORD®210 PLUS double beam spectrophotometer).

3. RESULTS AND DISCUSSION

3.1 UV-Vis analysis

The PLAL-prepared ZnONPs' UV-visible absorption spectra were measured between 280 and 680 nm in wavelength. Figure 3 displays the colloidal ZnONPs sample's optical absorbance after it was synthesized at 200 pulses. The absorption spectra have a strong absorption band at about 284.5 nm, which is due to the nanostructure of the ZnO nanoparticles distribution. The observed absorption peak at 284.5 nm is in close agreement with the results found by Rashid et al. [11] for their synthesized ZnO NPs using PLAL. The existence of well-dispersed nanoparticles with quantum size effects is thus established. The slightly blue-shifted peak compared to ZnO NPs made via chemical methods [5] here implies smaller particle sizes and higher purity because of the clean nature of PLAL.

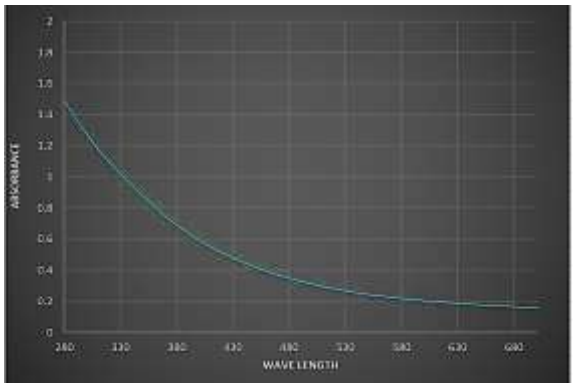

Figure 3. UV-Vis spectroscopy of ZnO nanoparticles

3.2 FE-SEM analysis

Figure 4(a) displays the ZnONPs FE-SEM images produced by laser ablation in DDW using 200 pulses and 600 mJ of laser energy. The resulting nanoparticles exhibit distinct needle-shaped morphology with Particle sizes ranging between 20-50 nm, also some nanoparticle clusters due to van der Waals forces. The characteristic needle-like shape of these particles is attributed to several key factors: Laser energy used (600 mJ), Number of laser pulses (200 pulses), and Properties of the liquid medium (deionized water).

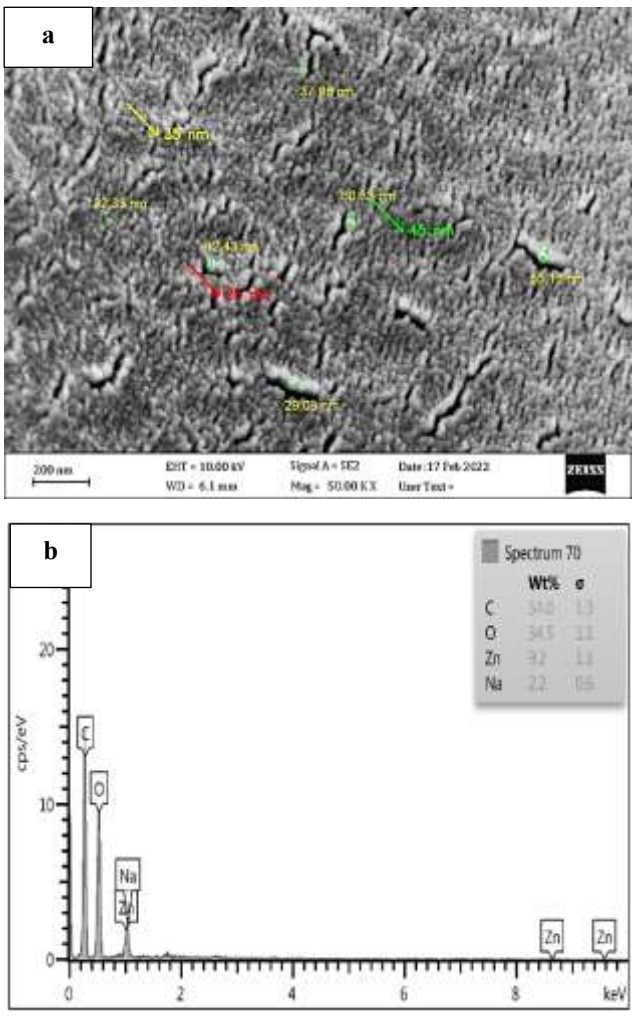

Figure 4. (a) FE-SEM image of ZnO nanoparticles and (b) EDX spectrum for ZnO colloidal elements

EDX analysis of ZnO colloidal, which includes Zn, O, C, and Na components in varying proportions, is shown in Figure 4(b). EDX Spectrum shows the chemical composition of the nanomaterial with distinct Zn peak at ~1.0 keV and ~8.6 keV and O peak at ~0.5 keV. The results indicate Zn/O ratio close to the theoretical expectation (1:1) and Presence of minor impurities attributed to Surface contamination during preparation and Residual components from the surrounding medium. Microscopic and chemical analysis of these nanoparticles confirm the successful laser ablation synthesis and explain the scientific basis of the antibacterial mechanism of these nanoparticles.

However, the morphology and size distribution in this study (20–50 nm, needle-like) agreed with the results given by the previous study [5], with their process being different from this study. Additionally, the morphology of cells in the current study was more uniform in comparison with previous studies, which is due to the rotational motion of the vessel and a selected laser fluence. EDX results are consistent with a near 1:1 Zn:O ratio, which conforms to the observations in Alwan et al. [12] where the PLAL synthesis of ZnO NPs offers minimal impurities.

3.3 XRD analysis

The XRD pattern as shown in Figure 5 exhibits characteristic diffraction peaks at 2θ positions of 31.78°, 34.47°, 36.26°, and 56.56°, which correlate to the (100), (002), (101), and (110) crystallographic planes, respectively. No extraneous peaks indicate that the samples have high purity, free of any detectable crystalline impurities. Observation of minor peaks at 12.2° and 22.5° is attributed to negligible secondary phases, which do not affect the properties of the material. The crystallite sizes as per the Scherrer Eq. (2) calculations vary from 50 to 65 nm, and this crystal size has important implications regarding antibacterial properties because the smaller crystals (closer to 50 nm) have higher surface areas that promote interaction with bacteria [21]. The XRD pattern showed sharp diffraction peaks that can be indexed to the hexagonal wurtzite structure, which agrees with the crystallographic features reported by Alwan et al. [22], Mohammed et al. [23], and Khalid et al. [24]. Additionally, crystallite sizes determined using the Scherrer equation (28–31 nm) are in agreement with the range reported by Swarnkar et al. [25], however, the slightly higher peak intensities indicate improved crystallinity here most likely due to controlled energy delivery and short ablation time. The higher surface area allows for the release of zinc ions, which are the main mechanism of antibacterial action in zinc oxide nanoparticles. The interaction of these ions with phosphate and sulfide groups causes disruption of bacterial cell membranes and generation of ROS, which causes oxidative stress and bacterial DNA damage.

$$D = \frac{k\lambda}{\beta \cos\theta} \quad (2)$$

Specific peaks (especially at 43.26°) show an enhanced intensity, characteristic of crystal growth orientation due to the preferred enhancement of the energy source during deposition techniques such as laser ablation.

The results of XRD confirm the complete laser-assisted synthesis of ZnO nanoparticles with high purity and the most optimal crystalline structure, and they have great potential in different biomedical applications.

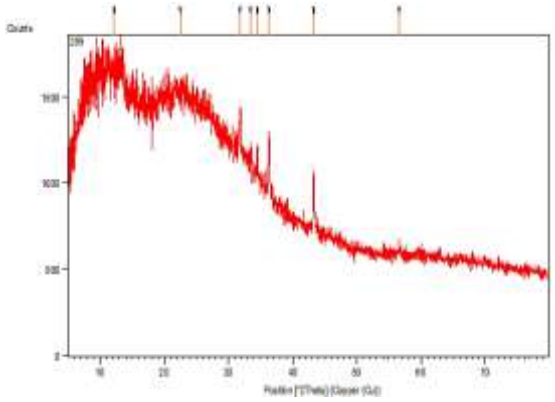

Figure 5. XRD pattern for a ZnO sample using a 600 mJ laser energy and a 200-laser pulse

3.4 Antibacterial activity

Figure 6 presents the results of antibacterial activity testing for zinc oxide nanoparticles against two bacterial strains, Escherichia coli (E. coli) (Gram-negative) and Staphylococcus aureus (S. aureus) (Gram-positive). Clear inhibition halos around wells containing nanoparticles indicate Halo diameter (Antibacterial effect intensity) and Halo clarity (Material's growth inhibition efficacy). The various bacterial types have different values of cell wall sensitivity (Gram-negative vs Gram-positive), which reflects the size variation. Zinc oxide nanoparticles show differential bacterial sensitivity between Gram-positive and Gram-negative bacteria.

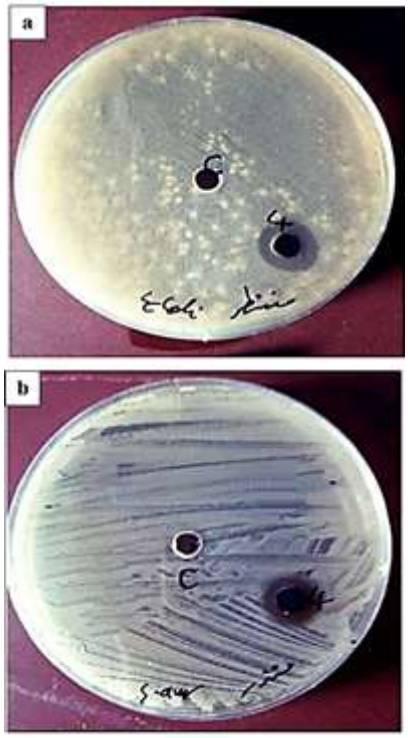

Figure 6. Antibacterial activity of laser-ablated ZnO NPs against (a) E. coli and (b) S. aureus demonstrated by well diffusion assay

This antibacterial effect (Figure 6) can be explained by two complementary mechanisms: the release of Zn^{2+} ions, which disrupt bacterial membranes and intracellular processes, and the generation of reactive oxygen species (ROS), which cause oxidative stress and damage to proteins, lipids, and DNA. The slightly higher inhibition zone observed for S. aureus compared to E. coli is attributed to the porous nature of the Gram-positive cell wall, which facilitates ion penetration and ROS activity, whereas the outer membrane of Gram-negative bacteria provides partial resistance.

This research supports further biomedical applications in antimicrobial therapy. According to here observed antibacterial activity of ZnO NPs, inhibition zones up to 25 and 20 mm are observed towards S. aureus and E. coli, respectively, which is comparable or even higher than that reported in Salih et al. [20] for chemically synthesized ZnO NPs. The results of this study may, in addition, be due to smaller size, higher crystallinity, and needle-like morphology increasing the surface contact with bacterial membranes and increasing the rate of Zn^{2+} ion release.

A clear trend in ZnO NPs antibacterial activity could be found correlated to the size in the data presented in Table 1 and Figure 7. For S. aureus and E. coli, it was also found that the inhibition zone was significantly larger on smaller nanoparticles that were 20–30 nm, also near 25 ± 1.2 mm and 20 ± 1.5 mm, respectively, at 50 µL. On the other hand, much-reduced activity (> 50 nm) was demonstrated, with zones of 12 ± 0.5 mm for 12 nm particles and 8 ± 0.8 mm for 8 nm particles, respectively. The size aspect correlation is derived from these two critical factors: 1) Enhanced Surface Area to Volume Ratio which can be shown in Eq. (3) [26] where it is sebematd that the smaller the radii of the particles, the higher the SAV ratio is and hence Increased Zn^{2+} ion release and 2) The Knudsen coefficient which depends on the radius of the particle, hence the smaller the radius, the greater is the correlation and Elevated reactive oxygen species (ROS) production [26, 27].

$$\mathrm{SAV} = \frac{3}{r} \tag{3}$$

where, r is the radius of the particle.

Table 1. ZnO NPs' inhibition zone diameters against S. aureus and E. coli at various particle sizes

Particle Size (nm)	Inhibition Zone (mm) for E. coli	Inhibition Zone (mm) for S. aureus	Concentration Used
20–30	20 ± 1.5	25 ± 1.2	50 µL (50 mg/10 mL)
30–50	15 ± 1.0	20 ± 1.0	50 Ml
>50	8 ± 0.8	12 ± 0.5	50 Ml

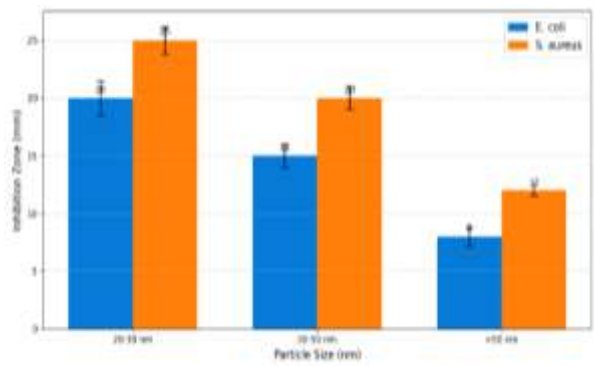

Figure 7. Size-dependent antibacterial activity of ZnO nanoparticles: Zones of inhibition for S. aureus and E. coli

4. CONCLUSION

The pulsed laser ablation in liquid (PLAL) method was successfully employed to synthesize Zinc Oxide Nanoparticles (ZnO NPs) with needle-like morphology, high crystallinity, and small particle size (20–50 nm). FE-SEM and XRD analyses confirmed their structural integrity and high purity, while UV-Vis spectroscopy revealed a characteristic absorption band at 284.5 nm. The antibacterial evaluation demonstrated significant inhibition zones up to 25 ± 1.2 mm for S. aureus and 20 ± 1.5 mm for E. coli, with higher efficiency than many chemically synthesized counterparts.

Beyond demonstrating their structural and antibacterial properties, the findings of this study suggest several promising biomedical applications for PLAL-synthesized ZnO NPs. Their strong antibacterial performance highlights their potential use in wound healing dressings, antimicrobial coatings for medical devices, and protective surface layers in hospital environments. Furthermore, due to their high purity and eco-friendly synthesis, these nanoparticles can be further explored for applications in drug delivery systems, biosensors, and photocatalytic disinfection in healthcare settings.

In summary, this work confirms that controlling nanoparticle morphology through PLAL not only enhances antibacterial efficiency but also opens new directions for ZnO NPs in safe, sustainable, and effective biomedical applications.

REFERENCES

[1] Alwan, A.M., Mohammed, M.S., Shehab, R.M. (2020). The performance of plasmonic gold and silver nanoparticle-based SERS sensors. Iraqi Journal of Science, 61(6): 1320-1327. https://doi.org/10.24996/ijs.2020.61.6.10

[2] Aghdam, H.D., Azadi, H., Esmaeilzadeh, M., Bellah, S.M., Malekfar, R. (2019). Ablation time and laser fluence impacts on the composition, morphology and optical properties of copper oxide nanoparticles. Optical Materials, 91: 433-438. https://doi.org/10.1016/j.optmat.2019.03.027

[3] Husham, K.A.F., Khdier, H.M., Saadoon, N.M., Ahmed, A. M. (2024). Preparation of CuO/PVA nanocomposite thin films for gamma ray attenuation via PLA method. Journal of Nanostructures, 14(3): 712-722. https://doi.org/10.22052/JNS.2024.03.002

[4] Ajaj, K., Al-Jubbori, M.A., Ali, A.M. (2023). Influence of ultraviolet irradiation on the optical properties and biological activity of copper nanoparticles prepared by pulsed laser ablation. Journal of Laser Applications, 35(4): 042055. https://doi.org/10.2351/7.0001221

[5] Mohammed A.K., Rafid M.A., Nedaa Y. (2024). Preparation ZnO nanoparticles with different concentration by laser ablation in liquid and their use in anti bacterial activity. Academic Science Journal, 2(1): 79-98. https://doi.org/10.24237/ASJ.02.01.835C

[6] Shehab, R.M., Alwan, A.M. (2023). Improved the sensitivity and limit of detection of surface alloying SERS sensors by controlling mixing ratio of trimetallic (Ag-Au-Pd) nanoparticles. International Journal of Nanoelectronics and Materials, 16(2): 359-370. https://doi.org/10.58915/ijneam.v16i2.1234

[7] Loera-Valencia, R., Neira, R.E., Urbina, B.P., Camacho, A., Galindo, R.B. (2022). Evaluation of the therapeutic efficacy of dressings with ZnO nanoparticles in the treatment of diabetic foot ulcers. Biomedicine and Pharmacotherapy, 155: 113708. https://doi.org/10.1016/j.biopha.2022.113708

[8] Wafi, A., Khan, M.M. (2025). Green synthesized ZnO and ZnO-based composites for wound healing applications. Bioprocess and Biosystems Engineering, 48(4): 521-542. https://doi.org/10.1007/s00449-024-03123-z

[9] Kareem, M.M. (2021). The effect of laser shots on morphological and optical properties of copper oxide NPs prepared by Nd-Yag laser of 1064 nm wavelengths in distilled water. Passer Journal of Basic and Applied Sciences, 3(2): 200-206. https://doi.org/10.24271/psr.33

[10] Adnan, N.N., Ab Razak, S.N., Roslan, M.S., Taib, N.A. M., Nurhafizah, H., Amran, N.B. (2020). Pulsed laser ablation produced copper nanoparticles (CUO NPS): The influence of time. Solid State Phenomena, 307: 279-284. https://doi.org/10.4028/www.scientific.net/SSP.307.279

[11] Rashid, S.N., Aadim, K.A., Jasim, A.S., Hamad, A.M. (2022). Synthesized zinc nanoparticles via pulsed laser ablation: Characterization and antibacterial activity. Karbala International Journal of Modern Science, 8(3): 462-476. https://doi.org/10.33640/2405-609X.3240

[12] Alwan, A.M., Mohammed, M.S., Shehab, R.M. (2020). Optimizing plasmonic characteristics of Ag-AuNPs/nanohillocks Si heterostructures for efficient SERS performance. International Journal of Nanoelectronics and Materials, 13(2): 323-340.

[13] Alwan, A.M., Mohammed, M.S., Shehab, R.M. (2021). Modified laser-etched silicon covered with bimetallic Ag–Au Alloy nanoparticles for high-performance SERS: Laser wavelength dependence. Indian Journal of Physics, 95(9): 1843-1851. https://doi.org/10.1007/s12648-020-01845-w

[14] Ahmed, A.M., Shehab, R.M., Hammed, M.A.N., Khalid, G.A., Jaber, G.S., Zaidan, M.A. (2025). Optimization of copper oxide nanoparticles production by pulsed laser ablation: A study on energy density effects. Annales de Chimie - Science des Matériaux, 49(2): 157-162. https://doi.org/10.18280/acsm.490206

[15] Afan, H.A., Aldlemy, M.S., Ahmed, A.M., Jawad, A.H., Naser, M.H., Homod, R.Z., Mussa, Z.H., Abdulkadhim, A.H., Scholz, M., Yaseen, Z.M. (2022). Thermal and hydraulic performances of carbon and metallic oxides-based nanomaterials. Nanomaterials, 12(9): 1545. https://doi.org/10.3390/nano12091545

[16] Ahmed, A.M., Rahmah, M.I. (2025). Synthesis and evaluation of PVP-stabilized platinum-doped ZnO nanoparticles: A dual approach for photocatalytic and antibacterial applications. BioNanoScience, 15(3): 332. https://doi.org/10.1007/s12668-025-01977-5

[17] Alwan, A.M., Shehab, R.M. (2015). Characterization of (nanostructures silver/silicon nano porous) active substrates for surface enhanced raman scattering (SERS) as a function to porous silicon parameters. Engineering and Technology Journal, 33(3): 556-563.

[18] Subhan, A., Mourad, A.H.I., Al-Douri, Y. (2022). Influence of laser process parameters, liquid medium, and external field on the synthesis of colloidal metal nanoparticles using pulsed laser ablation in liquid: A review. Nanomaterials, 12(13): 2144. https://doi.org/10.3390/nano12132144

[19] Shoeib, M.A., Abdelsalam, O.E., Khafagi, M.G., Hammam, R.E. (2012). Synthesis of Cu2O nanocrystallites and their adsorption and photocatalysis behavior. Advanced Powder Technology, 23(3): 298-304. https://doi.org/10.1016/j.apt.2011.04.001

[20] Salih, A.A., Nazar, A., Haider, A.J. (2019). Antibacterial activity of ZnO nanoparticle prepared by pulsed laser ablation in liquid for biological sensor. In 2019 12th International Conference on Developments in eSystems Engineering, Kazan, Russia, pp. 726-729. https://doi.org/10.1109/DeSE.2019.00135

[21] Swarnkar, R.K., Singh, S.C., Gopal, R. (2009). Synthesis of copper/copper-oxide nanoparticles: Optical and structural characterizations. AIP Conference Proceedings, 1147(1): 205-210. https://doi.org/10.1063/1.3183432

[22] Alwan, A.M., Mohammed, M.S., Shehab, R.M. (2020). Optimization of an ultra-sensitive Ag core-Au shell nanoparticle/Si surface-enhanced Raman scattering (SERS) sensor. AIP Conference Proceedings, 2307(1): 020005. https://doi.org/10.1063/5.0032762

[23] Mohammed, S.A., Khashan, K.S., Jabir, M.S., Abdulameer, F.A., Sulaiman, G.M., et al. (2022). Copper oxide nanoparticle ‐ decorated carbon nanoparticle composite colloidal preparation through laser ablation for antimicrobial and antiproliferative actions against breast cancer cell line, MCF-7. BioMed Research International, 2022(1): 9863616. https://doi.org/10.1155/2022/9863616

[24] Khalid, G.A., Abdulmawjod, M.I., Al-Bayaty, A. (2024). A comprehensive analysis of respiratory patterns and physiological parameters in asthma, bronchitis, and croup. Electrical Engineering Technical Journal, 1(1): 35-49. https://doi.org/10.51173/eetj.v1i1.3

[25] Swarnkar, R.K., Singh, S.C., Gopal, R. (2011). Effect of aging on copper nanoparticles synthesized by pulsed laser ablation in water: Structural and optical characterizations. Bulletin of Materials Science, 34(7): 1363-1369. https://doi.org/10.1007/s12034-011-0329-4

[26] Majed, A.A., Khalid, G.A., Humadi, A.F. (2024). Portable uroflowmetry system with integrated software for home urinary monitoring. In 2024 International Conference on Electrical and Computer Engineering Researches Gaborone, Botswana, pp. 1-5. https://doi.org/10.1109/ICECER62944.2024.10920439

[27] Sadrolhosseini, A.R., Noor, A.S.B.M., Shameli, K., Mamdoohi, G., Moksin, M.M., Mahdi, M.A. (2013). Laser ablation synthesis and optical properties of copper nanoparticles. Journal of Materials Research, 28(18): 2629-2636. https://doi.org/10.1557/jmr.2013.244